Semi-analytical method of calculating the electrostatic interaction of colloidal solutions*

Hongqing Tian(田洪庆) and Zengju Lian(连增菊)†

Faculty of Science, Ningbo University, Ningbo 315211, *China*

(Received 24 July 2016; revised manuscript received 31 October 2016; published online 22 December 2016)

We present a semi-analytical method of calculating the electrostatic interaction of colloid solutions for confined and unconfined systems. We expand the electrostatic potential of the system in terms of some basis functions such as spherical harmonic function and cylinder function. The expansion coefficients can be obtained by solving the equations of the boundary conditions, combining an analytical translation transform of the coordinates and a numerical multipoint collection method. The precise electrostatic potential and the interaction energy are then obtained automatically. The method is available not only for the uniformly charged colloids but also for nonuniformly charged ones. We have successfully applied it to unconfined diluted colloid system and some confined systems such as the long cylinder wall confinement, the air–water interfacial confinement and porous membrane confinement. The consistence checks of our calculations with some known analytical cases have been made for all our applications. In theory, the method is applicable to any dilute colloid solutions with an arbitrary distribution of the surface charge on the colloidal particle under a regular solid confinement, such as spherical cavity confinement and lamellar confinement.

Keywords: Poisson–Boltzmann equation, like-charged attraction, basis function expansion, multipoint collection method

PACS: 78.20.Bh, 02.70.–c, 05.10.–a, 78.67.Bf **DOI:** 10.1088/1674-1056/26/1/017801

1. Introduction

Colloidal solutions have been studied intensively for a long time because they are widely applied in industrial processes, biotechnologies, foods, and so on. Assembling colloidal nanoparticles into ordered structures is essential to the fabrication of nano-materials with high performance in optical, electrical, and mechanical properties. Such ordered structures normally are realized by self-assembly of nanoparticles for the required motion to reach a minimum energy state due to the small length scale and interaction energy. The final assembling structure of the colloidal nanoparticles is greatly sensitive to the environmental boundaries. For example, a face-centered cubic (fcc) and/or hexagonal close packed (hcp) crystal structure may be stacked from a bulk colloid solution,[1–7] an equilibrium hexatic phase or two-dimensional colloidal monolayer can be assembled of stably trapped colloidal particles at the air–water interface[8–12] and more complex 3D structures are obtained by confinement of the cylinder.[12–17] The mechanism of such self-assembling behavior greatly relies on the effective interaction of the system. The fundamental element of this interaction is obviously the effective interaction between two individual colloidal nanoparticles and/or between the particle and the confined wall.

Derjaguin *et al.*,[18,19] in their pioneering work, showed that the pair interaction between the charged colloids is dominated by the repulsive electrostatic interaction and the attractive van der Waals force (DLVO theory). Their theory has been widely adopted for the modelling and interpretation of the colloidal interactions and it has gained some extent success. However, more in-depth theoretical and experimental studies reveal that the DLVO theory works only for infinitely diluted particle solutions and long inter-particle separation. Moreover, there are experimental indications of an attractive long-ranged lateral interaction which is intrinsically electrostatic rather than a van der Waals nature.[20–22] These experiments ignited intensive interest in the study of the electrostatic interaction between like-charged colloids in bulk or confined conditions in recent decades. Carnie *et al.* calculated forces between identical or dissimilar spherical colloidal particles using nonlinear/linear Poisson–Boltzmann theory (NPB/LPB).[23–25] Several years later, Ospeck and Fraden solved the NPB equation using a similar method for two cylinders confined by two parallel charged plates and analyzed the confinement effects on the electrostatic repulsion of the particles, the screen length, and the effective surface charges on the particles.[26] In the same year, Bowen *et al.* investigated the solution with two spherical colloids under cylindrical confinement and obtained an attractive pair interaction.[27] However, it was soon proven by Neu *et al.* that this model cannot predict attraction and there must be a numerical error in Bowen's calculation.[28–30] All the above calculations of the pair interaction between the col-

*Project supported by the National Natural Science Foundation of China (Grant No. 11304169), the Natural Science Foundation of Ningbo City, China (Grant No. 2012A610178), the Open Foundation of the Most Important Subjects of Zhejiang Province, China (Grant No. xkzwl1505), and K. C. Wong Magna Fund in Ningbo University of China.

†Corresponding author. E-mail: lianzengju@nbu.edu.cn

© 2017 Chinese Physical Society and IOP Publishing Ltd

loids are numerical. The non-linearized Poisson–Boltzmann equation cannot be solved analytically for a spherical geometry or/and other nontrivial confinements. Even under the linear Poisson–Boltzmann (LPB) approximation, it is still difficult to obtain an analytical solution of the interaction energy between two colloidal particles under confined conditions.

In the present paper, we present a semi-analytical method of calculating the electrostatic interaction between colloidal spheres under the LPB approximation and apply this method to the unconfined system and confined systems such as cylinder confinement and air–water confinement. So far, in most studies, the colloid is assumed to be with fixed surface charge or even with fixed surface potential. While, many experimental indications show that the colloids may be nonuniformly charged and this inhomogeneity may be one of the important reasons inducing the anomalous "like-charged" attraction between colloids observed in experiments.[9,31,32] Our semi-analytical method is also available for this situation and we will elaborate the nonuniformly charge-induced "like-charged" attraction in Section 3.

2. The semi-analytical method

We consider a universal colloid system: two spherical colloids with radius R_1 and R_2 immersed in an electrolyte under a wall confinement with an arbitrary shape or trapped in an interface. The electrolyte is defined by specification of a temperature T, a total volume V, and chemical potentials for each kind of ion, μ_i (i is the i-th type of the ions). So, the ensemble that we work in is the grand-canonical ensmeble with the grand potential Ω. For convenience, we divide the system into two regions: one region is in the colloids and the other is out of the colloids. In the remainder of the paper, we use an "in" ("out") index to refer to the evaluation in (out) of the colloids. We set two parallel spherical coordinate systems on the center of two colloids, (r_i, θ_i, ψ_i), $i = 1, 2$, and one cylindrical coordinate system on the center of the confined boundary, (ρ, ψ, z). We present the formulation in a dimensionless way unless explicitly specified. All the lengths are in units by one of the colloid radius R_1, the charge is in units of the elementary charge e and the electric potential is dimensionless by multiplying $1/e\beta = k_{\mathrm{B}}T/e$ with the Boltzmann constant k_{B}.

The spherical colloids are assumed to be surface charged. The distribution of the surface charge can be arbitrary. Whatever it is, we can expand it in terms of the spherical harmonics, i.e.,

$$\sigma_i(\theta_i, \psi_i) = \sum_{s=0}^{+\infty} \sum_{t=-s}^{s} G_{st}^{(i)} Y_{st}(\theta_i, \psi_i), \quad i = 1, 2. \tag{1}$$

Since the charge is distributed only on the colloid surface, the electrostatic potential inside the colloid satisfies the Laplace equation,

$$\nabla^2 \Phi_{\mathrm{in}}^i(\boldsymbol{r}_i) = 0, \quad i = 1, 2. \tag{2}$$

Under the mean field approximation and a weak potential limit, the electrostatic potential outside the colloids can be well described by the linear Poinsson–Boltzmann theory. For a symmetric 1 : 1 electrolyte system, it has the form of

$$\nabla^2 \Phi_{\mathrm{out}}(\boldsymbol{r}) - \kappa^2 \Phi_{\mathrm{out}}(\boldsymbol{r}) = 0. \tag{3}$$

Here $\kappa = \sqrt{2z^2 c_0 \lambda_{\mathrm{B}}}$ with the Bjerrum length $\lambda_{\mathrm{B}} = e^2\beta/\varepsilon_{\mathrm{out}}R_1$ is the inverse screening length in the electrolyte. $\varepsilon_{\mathrm{out}}$ denotes the dielectric constant of electrolyte, z is defined as the valence of the ions in the electrolyte and c_0 is the dimensionless concentration (in units of $1/R_1^3$) of ions at the reference point where $\Phi_{\mathrm{out}}(\boldsymbol{r}) = 0$.

Due to the linear approximation, the potential outside the particles can be written as a superposition of three contributions: two charged colloidal spheres and the charged confined boundary. After solving Eqs. (3) and (2), we can obtain the electric potential of every contribution inside and outside the colloids expanded in terms of basis functions. Then, the potentials of the system read

$$\Phi_{\mathrm{in}}^i(\boldsymbol{r}_i) = \sum_{s=0}^{+\infty} \sum_{t=-s}^{s} C_{st}^i r_i^s Y_{st}(\theta_i, \psi_i), \quad i = 1, 2, \tag{4}$$

$$\begin{aligned} \Phi_{\mathrm{out}}(\boldsymbol{r}) = & \sum_{s=0}^{+\infty} \sum_{t=-s}^{s} A_{st} \mathcal{R}_s(r_1) Y_{st}(\theta_1, \psi_1) \\ & + \sum_{s=0}^{+\infty} \sum_{t=-s}^{s} B_{st} \mathcal{R}_s(r_2) Y_{st}(\theta_2, \psi_2) + \sum_{m=-\infty}^{+\infty} \mathrm{e}^{\mathrm{I}m\psi} \\ & \times \int_0^{\infty} \mathrm{d}w D_m(w) J_{|m|}(w\rho)\, \mathrm{e}^{-\xi\sqrt{w^2+\kappa^2}z}. \end{aligned} \tag{5}$$

Here, I is the imaginary unit. The first two terms in Eq. (5) denote the contributions from the surface charges on the particles as a function of the standard spherical coordinate, the last term is the contribution from the charged confined boundary expressed in the cylindrical coordinate with $\xi = 1$ for $z > 0$ and $\xi = -1$ for $z < 0$. Here, $\mathcal{R}_s(r_i) = r_i^{-s}$ for nonpolar substance (such as the air) and $\mathcal{R}_s(r_i) = k_s(\kappa r_i)$ for electrolyte (such as the water) representing the modified spherical Bessel function of the second kind. $Y_{st}(\theta_i, \psi_i)$ is the spherical harmonic function and $J_{|m|}(wr)$ denotes the Bessel function.

The coefficients C_{st}^i, A_{st}, B_{st}, and D_m are determined by the boundary conditions of the electrostatic potential in the system. In general, the boundaries should satisfy: (i) the electrostatic potential should vanish at infinity, (ii) the electric potential should be continuous on all interfaces, (iii) the associated electric displacements perpendicular to all the interfaces correspond to the surface charge densities, and (iv) the given confined boundary conditions. The first condition is satisfied automatically by the electrostatic potentials expressed

by Eqs. (4) and (5). Thus, the coefficients are only determined by the last three conditions. We can follow the process in two steps. First, we express D_m as a function of A_{st} and B_{st} based on the boundary conditions of the confinement by using a translation-rotation transformation of the spherical coordinate and the orthonormality and closure of basis functions. This calculation is an analysis process. Then, we give the values of C^i_{st}, A_{st}, and B_{st} by applying the boundary conditions on the colloid surfaces using a numerical "multipoint collection method".[33] We next describe the above process in detail.

After applying a translation transformation on the spherical coordinate i to a new position which coincides with the spherical coordinate j ($j \neq i$), the expression of the electrostatic potential outside the particles can be rewritten as

$$\begin{aligned}\Phi_{\text{out}}(\boldsymbol{r}) &= \sum_{s=0}^{+\infty}\sum_{t=-s}^{s}\left(A_{st}\mathcal{R}_s(r_i)+\hat{B}_{st}\hat{\mathcal{R}}_s(r_i)\right)Y_{st}(\theta_i,\psi_i)\\ &\quad+\sum_{m=-\infty}^{+\infty}\mathrm{e}^{\mathrm{I}m\psi}\int_0^{\infty}\mathrm{d}wD_m(w)J_{|m|}(w\rho)\,\mathrm{e}^{-\xi\sqrt{w^2+\kappa^2}z},\\ &\quad i=1 \text{ or } 2. \end{aligned} \tag{6}$$

Here $\hat{\mathcal{R}}_s(r_i)=r_i^{-s}$ for nonpolar substance and, for the polar substance, $\hat{\mathcal{R}}_s(r_1)$ equals $i_s(\kappa r_1)$ for $r_i<d$ and equals $k_s(\kappa r_i)$ for otherwise with the center–center distance, d. $i_s(\kappa r)$ is the modified spherical Bessel function of the first kind. $\hat{B}_{st}$ associates with the coefficient B_{st}. It has the form of

$$\hat{B}_{st}=\begin{cases}\sum_{LM}B_{LM}W_{LM,st}\tilde{\mathcal{R}}_{L-s}(d)Y_{L-s,M-t}(\eta_i,\phi_i), & \text{for nonpolar substance,}\\ \sum_{LM\lambda\mu}B_{LM}\mathcal{W}_{LM,st,\lambda\mu}\tilde{\mathcal{R}}_{\lambda}(d)Y_{\lambda\mu}(\eta_i,\phi_i), & \text{for polar substance,}\end{cases} \tag{7}$$

with

$$W_{LM,st}=(-1)^{l-L}\left[\frac{4\pi(2L+1)!}{(2l+1)!(2L-2s+1)!}\right]^{\frac{1}{2}}(s\ t\ L-s\ M-t|LM), \tag{8}$$

$$\mathcal{W}_{LM,st,\lambda\mu}=(-1)^{t+M}\sqrt{4\pi(2\lambda+1)(2L+1)(2s+1)}\begin{pmatrix}s & L & \lambda\\ 0 & 0 & 0\end{pmatrix}\begin{pmatrix}s & L & \lambda\\ t & -M & \mu\end{pmatrix}. \tag{9}$$

Here, $\tilde{\mathcal{R}}_s(d)=d^{-s}$ for the nonpolar substance; for the polar substance, $\tilde{\mathcal{R}}_s(d)$ equals $k_s(\kappa d)$ for $r_i<d$, equals $i_s(\kappa d)$ otherwise. (d,η_i,ϕ_i) is a vector from the center of particle i to the center of particle j with respect to the spherical coordinate system (r_i,θ_i,ψ_i).

Substituting the electrostatic potential in Eq. (6) to the given confined boundary conditions, we can express D_m precisely as a function of the coefficients A_{lm} and B_{lm} ascribing to the orthonormality and closure of the Bessel functions and/or exponential functions.

$$D_m(w)=\hat{D}_m(w,A_{st},B_{st})/H(w). \tag{10}$$

The right hand of the above equation is in general a standard Hankel transform or Fourier transformation.

Now, we substitute the electrostatic potentials (4) and (6) into the boundary conditions on the sphere surfaces,

$$\Phi^i_{\text{in}}(\boldsymbol{r}_i)=\Phi_{\text{out}}(\boldsymbol{r}_i),\quad \boldsymbol{r}_i\in S_i,\quad i=1,2, \tag{11}$$

$$(\tau\nabla\Phi^i_{\text{in}}(\boldsymbol{r}_i)-\nabla\Phi_{\text{out}}(\boldsymbol{r}_i))\cdot\boldsymbol{n}_i=\lambda_{\text{B}}\sigma_i(\boldsymbol{r}_i),\quad \boldsymbol{r}_i\in S_i,\quad i=1,2, \tag{12}$$

where S_i represents the surface of particle i and $\boldsymbol{n}_i$ is the outer normal unit vector of S_i. $\sigma_i(\boldsymbol{r}_i)$ is the surface charged density of the i-th sphere. $\tau=\varepsilon_{\text{in}}/\varepsilon_{\text{out}}$ is the ratio between the dielectric constants of the particle and the fluid. Four linear functions associated with the coefficients $\{A_{st}\}$, $\{B_{st}\}$, $\{C^1_{st}\}$, and $\{C^2_{st}\}$ are yielded

$$\mathcal{F}_1(\{A_{st}\},\{B_{st}\},\{C^1_{st}\},\{C^2_{st}\},\theta_1,\psi_1)=0, \tag{13}$$

$$\mathcal{F}_2(\{A_{st}\},\{B_{st}\},\{C^1_{st}\},\{C^2_{st}\},\theta_1,\psi_1)=0, \tag{14}$$

$$\mathcal{F}_3(\{A_{st}\},\{B_{st}\},\{C^1_{st}\},\{C^2_{st}\},\theta_2,\psi_2)=0, \tag{15}$$

$$\mathcal{F}_4(\{A_{st}\},\{B_{st}\},\{C^1_{st}\},\{C^2_{st}\},\theta_2,\psi_2)=0. \tag{16}$$

Using the so-called "multipoint collection method", the coefficients $\{A_{st}\}$, $\{B_{st}\}$, $\{C^1_{st}\}$, and $\{C^2_{st}\}$ can be determined by substituting a discrete set of points on the spherical boundaries. The equations are solved by an iterative method. First, after an initial guess at the coefficients $\{A_{st}\}$, $\{B_{st}\}$, $\{C^1_{st}\}$, and $\{C^2_{st}\}$, we get the value of D_m from Eq. (10) through a Hankel or Fourier transformation. Then, by applying the "multipoint collection method" and inserting the obtained D_m into Eqs. (13)–(16), $\{A_{st}\}$, $\{B_{st}\}$, $\{C^1_{st}\}$, and $\{C^2_{st}\}$ are then obtained. These new results are used as input values for the next iteration. It should be noticed that, in the complete expansion in Eqs. (13)–(16), there are infinite numbers of coefficients to be determined, i.e., infinite numbers of points on the spherical surfaces are needed in a numerical calculation. Fortunately, in a real numerical calculation, the expansions can be truncated at some finite value, i.e., $s_{\max}=N$.

After obtaining the electrostatic potential of the system, the grand energy of the system reads

$$\beta\Omega=\frac{R_1}{2\beta\,\mathrm{e}^2}\int_V\mathrm{d}\boldsymbol{r}\varepsilon(\boldsymbol{r})\left[|\nabla\Phi_{\text{in}}(\boldsymbol{r})|^2+|\nabla\Phi_{\text{out}}(\boldsymbol{r})|^2\right]$$

$$+\sum_{j=\pm}\int_V \mathrm{d}\boldsymbol{r} n_j(\log n_j\Lambda^3-1)-\beta\mu\sum_{j=\pm}\int_V \mathrm{d}\boldsymbol{r} n_j. \quad (17)$$

Here, Λ and $n_\pm$ are the reduced thermal wavelength and dimensionless densities of positive and negative ions in the electrolyte, respectively. The last two terms are the entropies associated with ion distributions. The interaction energy of the system then can be obtained by minusing the energy when two particles go to infinity, $\beta\Omega_0$, i.e., $\beta\Omega_{\rm int}=\beta\Omega-\beta\Omega_0$. In the linear screening approximation, for the asymmetric 1 : 1 electrolyte system, the interaction energy can be rewritten as

$$\beta\Omega_{\rm int} = \frac{1}{2\lambda_{\rm B}}\left[\sum_{i=1,2}\int \mathrm{d}S_i\Phi_{\rm out}(\boldsymbol{r})\sigma_i(\boldsymbol{r}) + \int \mathrm{d}S_{\rm c}\Phi_{\rm out}\sigma_{\rm c}(\boldsymbol{r})\right]-\beta\Omega_0. \quad (18)$$

Here, S_i and $S_{\rm c}$ are the particle surface and the confined boundary surface, respectively. $\sigma_{\rm c}(\boldsymbol{r})$ denotes the charge distribution on surface $S_{\rm c}$.

3. Application of the method

3.1. Unconfined system

We first apply the method to the electrostatic interaction between two like-charged colloids in a dilute unconfined colloidal system. The colloids are nonuniformly charged with the same radius $R_1=R_2=R$. We consider a simple surface charge distribution like

$$\sigma_i=\sigma_0(1+b_0\cos(\theta_{0i})). \quad (19)$$

Here, θ_{0i} is the angle with respect to the i-th effective dipolar moment. b_0 and σ_0 are two arbitrary constants. After a rotation translation of σ_i, it can be expressed in (r_i,θ_i,ψ_i) as follows:

$$\sigma_i(\theta_{0i})=\begin{cases}\sigma_0[2\sqrt{\pi}Y_{0,0}(\theta_i,\psi_i) & \\ +\sqrt{\dfrac{4\pi}{3}}b_0Y_{1,0}(\theta_i,\psi_i)], & i=1,\\ \sigma_0[2\sqrt{\pi}Y_{0,0}(\theta_i,\psi_i) & \\ +\dfrac{4\pi}{3}b_0(Y_{1,0}(\gamma,\alpha)Y_{1,0}(\theta_i,\psi_i) & \\ -Y_{1,-1}(\gamma,\alpha)Y_{1,1}(\theta_i,\psi_i) & \\ -Y_{1,1}(\gamma,\alpha)Y_{1,-1}(\theta_i,\psi_i))], & i=2.\end{cases} \quad (20)$$

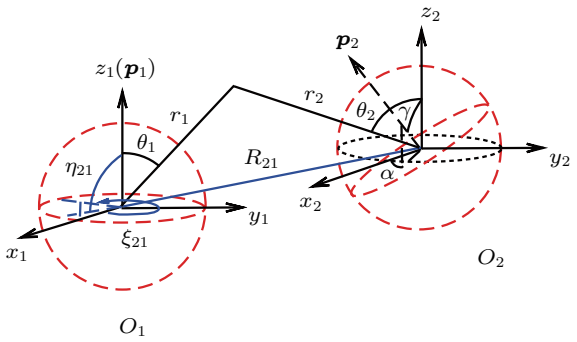


Fig. 1. (color online) Sketch of the system with two like-charged particles immersed in an electrolyte. Two parallel coordinates are set on the particle centers respectively. The effective dipolar moment of particle 1, $\boldsymbol{p}_1$, is along the z_1 axis and the dipolar vector $\boldsymbol{p}_2$ for particle 2 is denoted as (p,γ,α) with respect to spherical coordinates 2.

In this unconfined system, $D_m(w)=0$ in Eq. (5) which profoundly simplifies the calculation. Due to the orthogonality of the spherical harmonic function $Y_{st}(\theta,\psi)$, the linear equations (13)–(16) can be simplified as follows:

$$\sum_{lm\lambda\mu}B_{lm}\mathcal{W}_{lm,st,\lambda,\mu}k_\lambda(\kappa d)Y_{\lambda\mu}(\eta_j,\phi_j) = \frac{\left[\dfrac{\partial}{\partial r_1}k_s(\kappa r_1)|_{r_1=1}-\tau s k_s(\kappa)\right]A_{st}+\sigma_0(\dfrac{2}{3}\sqrt{3\pi}b_0\delta_{s1,t0}+2\sqrt{\pi}\delta_{s0,t0})}{\tau s i_s(\kappa)-\dfrac{\partial}{\partial r_1}i_s(\kappa r_1)|_{r_1=1}}, \quad (21)$$

$$\sum_{lm\lambda\mu}A_{lm}\mathcal{W}_{lm,st,\lambda,\mu}k_\lambda(\kappa d)Y_{\lambda\mu}(\eta_i,\phi_i) = \frac{\left[\dfrac{\partial}{\partial r_2}k_s(\kappa r_2)|_{r_2=1}-\tau s k_s(\kappa)\right]B_{st}+\dfrac{1}{3}\sqrt{6\pi}\sigma_0b_0(\mathrm{e}^{\mathrm{I}\alpha}\delta_{s1,t,-1}-\mathrm{e}^{-I\alpha}\delta_{s1,t1})\sin\gamma}{\tau s i_s(\kappa)-\dfrac{\partial}{\partial r_2}i_s(\kappa r_2)|_{r_2=1}} + \frac{\sigma_0(\dfrac{2}{3}\sqrt{3\pi}b_0\cos\gamma\delta_{s1,t0}+2\sqrt{\pi}\delta_{s0,t0})}{\tau s i_s(\kappa)-\dfrac{\partial}{\partial r_2}i_s(\kappa r_2)|_{r_2=1}}, \quad (22)$$

$$C^1_{st} = \frac{\left[i_s(\kappa)\dfrac{\partial}{\partial r_1}k_s(\kappa r_1)|_{r_1=1}-k_s(\kappa)\dfrac{\partial}{\partial r_1}i_s(\kappa r_1)|_{r_1=1}\right]A_{st}}{s\tau i_s(\kappa)-\dfrac{\partial}{\partial r_1}i_s(\kappa r_1)|_{r_1=1}} + \frac{i_s(\kappa)\sigma_0\left[\dfrac{2}{3}\sqrt{3\pi}b_0\delta_{s1,t0}+2\sqrt{\pi}\delta_{s0,t0}\right]}{s\tau i_s(\kappa)-\dfrac{\partial}{\partial r_1}i_s(\kappa r_1)|_{r_1=1}}, \quad (23)$$

$$C_{st}^2 = \frac{\left[i_s(\kappa)\frac{\partial}{\partial r_2}k_s(\kappa r_2)|_{r_2=1} - k_s(\kappa)\frac{\partial}{\partial r_2}i_s(\kappa r_2)|_{r_2=1}\right]B_{st} + \frac{2}{3}\sqrt{3\pi}\sigma_0 b_0 i_s(\kappa)\delta_{s1,t0}\cos\gamma}{\tau s i_s(\kappa) - \frac{\partial}{\partial r_2}i_s(\kappa r_2)|_{r_2=1}}$$
$$+ \frac{i_s(\kappa)\sigma_0\left[\frac{1}{3}\sqrt{6\pi}b_0(\mathrm{e}^{\mathrm{I}\alpha}\delta_{s1,t,-1} - \mathrm{e}^{-\mathrm{I}\alpha}\delta_{s1,t1})\sin\gamma + 2\sqrt{\pi}\delta_{s0,t0}\right]}{\tau s i_s(\kappa) - \frac{\partial}{\partial r_2}i_s(\kappa r_2)|_{r_2=1}}. \quad (24)$$

These four linear equations can be analytically solved as long as the indices s and l can be truncated, i.e., $s_{\max} = N_1$ and $l_{\max} = N_2$.

After solving the coefficients by the above four equations, the electrostatic potential of the system and the instantaneous interaction energy for a specified configuration of the two colloid spheres can be obtained by Eqs. (4), (5), and (18). It should be noticed that, in a real experiment, the colloid can rotate due to thermal agitations. An instantaneous interaction energy does not represent the experiment measured one. In order to get the experimental comparable results, we have to calculate the potential for all the possible orientations and average the results with a Boltzmann factor.

$$\beta\overline{\Omega}_{\mathrm{int}} = \frac{\int \mathrm{d}\omega\beta\Omega\,\mathrm{e}^{-\beta\Omega}}{\int \mathrm{d}\omega\,\mathrm{e}^{-\beta\Omega}} - \beta\Omega_0, \quad (25)$$

where ω denotes the angle position of the second sphere and relative orientation of the two spheres.

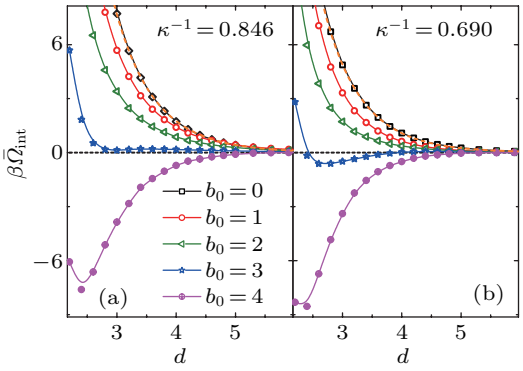


Fig. 2. (color online) The effective interaction energy as a function of the reduced colloid–colloid separation for uniformly and nonuniformly charged particles. The dashed lines in orange are the nonlinear fits with the screened Coulomb potential. The radius of the particle $R = 0.5$ μm and the total charges of one colloid $Q = 500$.

Figure 2 shows the results of the effective interaction between two like-charged colloid spheres after an average with the Boltzmann factor as given by Eq. (25). From this figure, we find that the interaction energy is sensitive to the distribution of the surface charge on the colloid. The electrostatic repulsion decreases with the increase of b_0 which characterizes the surface heterogeneity. Only when $b_0 = 0$, is the distribution of surface charge homogenous, otherwise, it is inhomogenous. The effective dipolar moment of the surface charge with the distribution in Eq. (19) is $\frac{4}{3}b_0\pi R^3\sigma_0$. Obviously, the effective dipolar moment increases linearly with b_0. So, figure 2 indicates further that the electrostatic repulsion weakens with the increase of the effective dipolar moment of the colloidal particle. When the effective dipolar moment is large enough, the electrostatic repulsion turns to attraction. This interesting result illustrates that the "like-charged" attraction is possible and it even exists in such an unconfined system as long as the colloid is nonuniformly charged and its dipolar moment is large enough. The critical value of the effective dipolar moment at which the interaction turns from repulsion to attraction is affected by the screen length of the water. Figure 2 shows that the critical dipolar moment is smaller for a shorter screen length. Meanwhile, the colloid characters, such as the size and the total charge, are other important roles in effect on the pair electrostatic interaction. For a detailed illustration, we refer to our early work.[34]

The orange dash lines in the figure are the nonlinear fits with the screened Coulomb potential for the case of the homogenously charged colloid. They fit well at the large colloidal separation which confirms the reliability of our calculation.

3.2. The colloid system with a cylinder confinement

Since the anomalous "like-charged" attraction is mostly found in a confined system in real experiments, we extend our calculation to the confined case and study the combined effect of the nonuniform charge distribution and the confinement on the interaction energy. Here, we consider a diluted colloid solution confined in a long charged cylinder wall (see Fig. 3).[33] We still use the same distribution in the above model in Eq. (19) to character the inhomogeneity of the surface charge on the colloid.

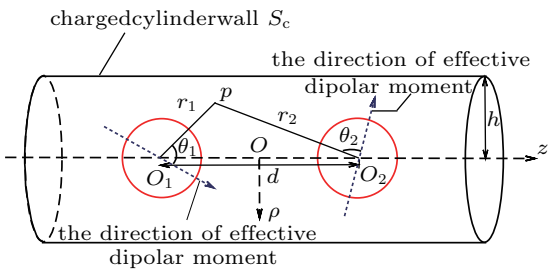


Fig. 3. (color online) Sketch of the system with two charged spheres immersed in electrolyte confined in a cylindrical wall.

The boundary conditions of the cylinder wall are associated with its physical or/and chemical characters. Two kinds of walls are usually used in the experiment: one is the glass[35–37] and the other is a conductor.[38] These two walls can be modeled by two simple boundaries: the fixed surface charge model and the fixed surface potential model.

The calculation procedures of the interaction energy for these two models are similar but they have different specific formulaes for the $D_m(w)$ in Eq. (10). For the model of the fixed surface potential boundary of the cylinder wall, $H(w)$ and $\hat{D}_m^{\pm}(w,A_{lm},B_{lm})$ have the forms of

$$\begin{aligned}&\hat{D}_m(w,A_{st},B_{st})\\&=-\int_0^{\xi\infty}\int_0^{2\pi}\mathrm{d}z\mathrm{d}\psi\Bigg[\sum_{s,t}A_{s,t}k_s(\kappa r_1)Y_{s,t}(\theta_1,\psi_1)|_{\rho=h}\\&+\sum_{s,t}B_{s,t}k_s(\kappa r_2)Y_{s,t}(\theta_2,\psi_2)|_{\rho=h}\Bigg]\\&\times\mathrm{e}^{-(\xi\sqrt{w^2+\kappa^2}z+\mathrm{I}m\psi)},\end{aligned}\tag{26}$$

$$H(w)=-4\pi^2J_{|m|}(wh).\tag{27}$$

While, for the fixed surface charge case, they read

$$\begin{aligned}&\hat{D}_m(w,A_{st},B_{st})\\&=\int_0^{\xi\infty}\int_0^{2\pi}\mathrm{d}z\mathrm{d}\psi\Bigg\{\Bigg[\sum_{s,t}A_{s,t}k_s(\kappa r_1)Y_{s,t}(\theta_1,\psi_1)|_{\rho=h}\\&+\sum_{s,t}B_{s,t}k_s(\kappa r_2)Y_{s,t}(\theta_2,\psi_2)|_{\rho=h}\Bigg]\tau_{\mathrm{c}}\partial K_{|m|}(w\rho)/\partial\rho|_{\rho=h}\\&-K_{|m|}(wh)\Bigg[\sum_{l,m}A_{l,m}\partial[k_l(\kappa r_\alpha)Y_{l,m}(\cos\theta_\alpha,\psi_\alpha)]/\partial\rho|_{\rho=h}\\&+\sum_{l,m}A_{l,m}\partial[k_l(\kappa r_\alpha)Y_{l,m}(\cos\theta_\alpha,\psi_\alpha)]/\partial\rho|_{\rho=h}-\sigma_{\mathrm{c}}\Bigg]\Bigg\}\\&\times\mathrm{e}^{-(\xi\sqrt{w^2+\kappa^2}z+\mathrm{I}m\psi)},\end{aligned}\tag{28}$$

$$\begin{aligned}H(w)&=K_{|m|}(wh)\partial J_{|m|}(w\rho)/\partial\rho|_{\rho=h}\\&\quad-J_{|m|}(wh)\tau_{\mathrm{c}}\partial K_{|m|}(w\rho)/\partial\rho|_{\rho=h}.\end{aligned}\tag{29}$$

Here, τ_{c} is the dielectric constant ratio between the cylinder wall and water. $K_{|m|}(|w|\rho)$ is the modified Bessel function of the second kind. The coordinates of two spherical systems and the cylinder system have the relationship with

$$r_1=\sqrt{\rho^2+(z+d)^2},\tag{30}$$

$$r_2=\sqrt{\rho^2+(z-d)^2},\tag{31}$$

$$\cos\theta_1=(z+d)/\sqrt{\rho^2+(z+d)^2},\tag{32}$$

$$\cos\theta_2=(z-d)/\sqrt{\rho^2+(z-d)^2}.\tag{33}$$

In general, equations (26) and (28) are the two dimensions Fourier transforms. When the effective dipolar moment of the colloids are parallel with the symmetry axis of the cylinder wall (parallel case), the system has a cylindrical symmetry. Then, the Fourier transforms can reduce to one dimension. Once getting the specific expressions of $D_m(w)$ and $H(w)$, the electrostatic potential and the interaction energy can be obtained by solving Eqs. (13)–(16) and (18).

A comparison of interaction energies with various sphere–wall separations, h, is shown in Fig. 4. In the case of the fixed potential model, the interaction energy increases with h for the four different distributions of surface charges on the spheres, $b_0=0$, $b_0=1$, $b_0=1.7$, and $b_0=2$. While, for the fixed charge density model, the situation is opposite. Interestingly, whatever the boundary condition of the cylinder wall is, the interaction energy tends to the unconfined case. For the case of an unconfined system denoted by a solid line and the case of $h=10$ for both the fixed potential model and the fixed charge density model, they are superposed and hardly distinguishable. This provides a consistency check of our calculations. Like the case of the unconfined system, the figure also suggests that the interaction energy changes quantitatively and qualitatively with the heterogeneity parameter of the surface charge on the particle, b_0. It is most noticeable that the reduction of the sphere–wall separation also qualitatively changes the interaction energy for both $b_0=1.7$ and $b_0=2$ in Figs. 4(c) and 4(d). It suggests that the cylindrical confinement is another important reason to cause the "like-charged" attraction.

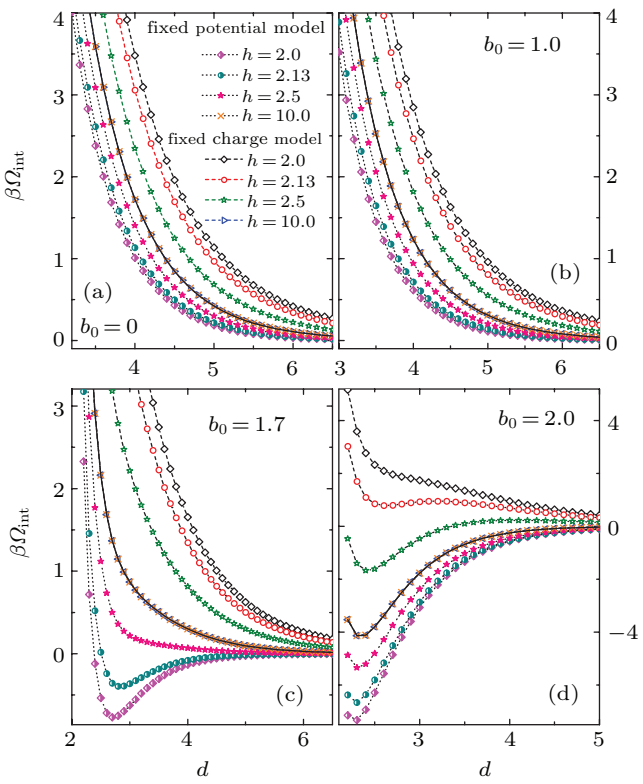


Fig. 4. (color online) The interaction energy of two spheres as a function of the colloid–colloid distance with different sphere–wall separations h for two models of the boundary conditions on the cylinder wall. The solid line is the case of the unconfined system. The other parameters of the system are $R=0.5$ μm, $Q=500$, and $\kappa^{-1}=0.846$.

3.3. The interfacial colloid system

The study of the system with colloidal particles trapped at the air–water interface has caused intensive interest for a long time because such system can easily assemble a colloidal monolayer. This monolayer is an interesting model system for exploring physical bases in reduced dimensions and because they can be used to engineer novel materials.

After the pioneering work by Pieranski,[39] it is widely recognized that the electrostatic interaction between two particles trapped in an air–water interface involves mainly two components: the Coulombic contribution and the dipolar contribution.[40,41] The former term arises from the overlap of diffuse layers in the gap between neighboring particles. The latter term is due to an asymmetric counterion cloud surrounding each particle as a consequence of the asymmetric dielectric medium (air/water). After the assumption of point particle and linear Poisson–Boltzmann approximation, Hurd[42] gave asymptotic forms of the inter-particle energy

$$\beta\Omega_{\rm int} = A\,{\rm e}^{-\kappa d}/d + Bd^{-3}. \tag{34}$$

Hurd's calculation turns out that, for a large inter-particle separation ($\kappa d \gg 10$), the power-law dipolar contribution dominates the interaction and it decays asymptotically $\propto 1/d^3$. The prefactors A and B in Eq. (34) determine the magnitudes of the screened Coulomb interaction and the dipole–dipole interaction. They depend on the effective charges of the particles and the effective dipole moments caused by their surrounding counterions, respectively. The dipole moment caused by the asymmetric dielectric medium is perpendicular to the interface, thus $B > 0$. However, considering the nonuniform distribution of the surface charge on the particle, the dipole moment may orient diagonally with respect to the air–water interface with an angle α. Unfortunately, this situation is rarely considered in either Hurd or others' works. Noticeably, the counterions associated with the particles can arrange themselves and spread uniformly around the particle even though the particles are weakly nonuniformly charged. Thus, for weakly anisotropic distribution of the surface charge on the colloid, the corresponding effective dipole moment may still be perpendicular to the interface.[43] While, for strongly anisotropic distribution of the surface charge, such as so-called "Janus-like" charged colloids (positive and negative charges coexist in different patches on the colloid surface), the possibility of an effective dipole moment oriented diagonally with respect to the interface is foreseeable. When the angle α reaches a critical point at which the parallel dipole–dipole interaction translates from the repulsion to the attraction, finally, the coefficient B may be less than zero. This implies that the like-charged particles trapped in the air–water interface may attract each other. Such inter-colloidal attraction was also indicated in the metastable mesostructures at the aqueous interface in many experiments.[9,10,31,44] Some researches attributed this attraction to other reasons, such as, the capillary interaction.[45–49] However, a complete and final picture has not yet been reached.

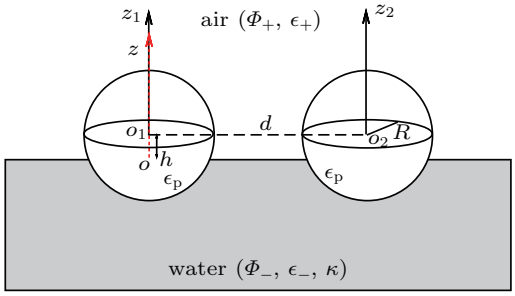


Fig. 5. (color online) Sketch of two charged spherical colloids trapped in an air–water interface. Three coordinate systems are set in the system: two parallel spherical coordinates whose origins are fixed on the center of the colloids and one cylindrical coordinate whose origin is fixed on the center of the first particle-interface intersecting plane. The flat interface is on $z = 0$ and separates an upper air phase (dielectric constant ε_+) from a lower electrolytic phase (dielectric constant ε_-). Two colloids are trapped in the air–water interface with a center–interface distance h and the center–center distance d.

We apply the above semi-analytical calculation in an interfacial system with two nonuniformly like-charged colloids (see Fig. 5).[50] The colloids are trapped in the air–water interface with a center–interface distance h. The colloidal spheres are assumed to be surface charged. The charges usually result from the dissociation of chemical groups on the particles in the polar substance. Thus, the distribution of the charges must be asymmetric with respect to the reflection in the plane of the interface since the chemical groups cannot dissociate in a nonpolar substance. Meanwhile, the charge on the water–colloid surface is not always distributed uniformly for the possible renormalizing of the chemical groups immersed in the water. Moveover, negative and positive ions may be both dissociated from different chemical groups (it is common for biocolloid). It means that positive and negative patches may coexist on the colloid surface forming so-called "Janus" particles. We assume a simple form to describe this asymmetry,

$$\sigma_i^+(R,\theta_i,\psi_i) = 0, \quad \boldsymbol{r}_i \in S_i^+, \tag{35}$$

$$\sigma_i^-(R,\theta_i,\psi_i) = \sigma_0(1+\varsigma b_1 + b_1\cos 2\theta_i)(1+b_2\cos\psi_i), \quad \boldsymbol{r}_i \in S_i^-, \tag{36}$$

with $\varsigma = (1+3\cos\beta - 2\cos^3\beta)/3(1+\cos\beta)$ and $\sin\beta = h/R$. Here, $\sigma_i^{\pm}(R,\theta_i,\psi_i)$ are defined as the surface–charge distributions on the particle i. In the remainder of the paper, the $+$ $(-)$ index will refer to evaluation in the air (water) phase. S_i represents the surface of particle i. σ_0 is the average surface charge density. b_1 and b_2 are adjustable parameters characterizing the surface heterogeneity. The additional term of ς ensures the total charge of the particle is independent of the coefficients

b_1 and b_2. Then, the total charge of the particle then can be expressed as $Q_i = \int \mathrm{d}S\sigma_i^{\pm}(R,\theta_i,\psi_i) = 2\pi R^2\sigma_0(1+\cos\beta)$.

Because the system is divided into an air phase and a water phase, the electrostatic potential outside the colloidal particles in Eq. (5) should be rewritten as follows:

$$\begin{aligned}\Phi_{\mathrm{out}}^{\pm}(\boldsymbol{r}) &= \sum_{s=0}^{+\infty}\sum_{t=-s}^{s} A_{st}^{\pm}\mathcal{R}_s^{\pm}(r_1)Y_{st}(\theta_1,\psi_1)\\ &+\sum_{s=0}^{+\infty}\sum_{t=-s}^{s} B_{st}^{\pm}\mathcal{R}_s^{\pm}(r_2)Y_{st}(\theta_2,\psi_2)\\ &+\sum_{m=-\infty}^{+\infty}\mathrm{e}^{\mathrm{I}m\psi}\int_0^{\infty}\mathrm{d}wD_m^{\pm}(w)J_{|m|}(wr)\,\mathrm{e}^{-w_{\pm}z}, \quad (37)\end{aligned}$$

with $w_{\pm} = \pm\sqrt{w^2+\kappa_{\pm}^2}$. Here, $\mathcal{R}_s^{+}(r_i) = r_i^{-s}$ for the upper region and $\mathcal{R}_s^{-}(r_i) = k_s(\kappa r_i)$ for the lower region. We assume a neutrality condition on the air–water interface. Then the boundary condition on the interface has the form of

$$\Phi_{\mathrm{out}}^{+}(\boldsymbol{r}) = \Phi_{\mathrm{out}}^{-}(\boldsymbol{r}) = 0, \quad \boldsymbol{r}\to\infty, \quad (38)$$

$$\frac{\partial\Phi_{\mathrm{out}}^{-}(\boldsymbol{r})}{\partial z} = \tau_{\mathrm{aw}}\frac{\partial\Phi_{\mathrm{out}}^{+}(\boldsymbol{r})}{\partial z}, \quad \boldsymbol{r}\notin V_i, \quad i=1,2, \quad z=0, \quad (39)$$

$$\Phi_{\mathrm{out}}^{-}(\boldsymbol{r}) = \Phi_{\mathrm{out}}^{+}(\boldsymbol{r}), \quad \boldsymbol{r}\notin V_i, \quad i=1,2, \quad z=0. \quad (40)$$

Here, τ_{aw} is the dielectric constant ratio between the air and the water. Obviously, the boundary condition of Eq. (38) is satisfied automatically for the potential with the above form of Eq. (37). The conditions of Eqs. (39) and (40) can be extended to the region in the particles by continuing the outside field $\phi_{\mathrm{out}}^{\pm}$ with a virtual solution into the interior of the particles and making $\tau_{\mathrm{aw}} = 1$ in the particles. Thus, we can express $D_m^{\pm}$ precisely as a function of the coefficients $A_{lm}^{\pm}$ and $B_{lm}^{\pm}$ in Eq. (10) ascribing to the orthonormality and closure of the Bessel functions $\{J_{|m|}(wr)\}$ and exponential functions $\{\mathrm{e}^{\mathrm{i}m\psi}\}$. Here,

$$\begin{aligned}&\hat{D}_m^{\pm}(w,A_{lm}^{\pm},B_{lm}^{\pm})\\ &= \int_0^{+\infty}\mathrm{d}rJ_{|m|}(wr)r\\ &\times\sum_l\Big[E_{lm}(r)\frac{\partial P_{lm}(z=r_1\cos\theta_1+h=0)}{\partial z}\\ &+G^{\pm}(w)Q_{lm}(r)P_{lm}(z=r_1\cos\theta_1+h=0)\Big], \quad (41)\end{aligned}$$

with

$$\begin{aligned}E_{lm}(r) &= \sqrt{\frac{(2l+1)(l-m)!}{4\pi(l+m)!}}(\tau_{\mathrm{aw}}(A_{lm}^{+}\mathcal{R}_l^{+}(r)+\hat{B}_{lm}^{+}\hat{\mathcal{R}}_l^{+}(r))\\ &-(A_{lm}^{-}\mathcal{R}_l^{-}(r)+\hat{B}_{lm}^{-}\hat{\mathcal{R}}_l^{-}(r))), \quad (42)\\ Q_{lm}(r) &= \sqrt{\frac{(2l+1)(l-m)!}{4\pi(l+m)!}}(A_{lm}^{+}\mathcal{R}_l^{+}(r)+\hat{B}_{lm}^{+}\hat{\mathcal{R}}_l^{+}(r)\\ &-A_{lm}^{-}\mathcal{R}_l^{-}(r)-\hat{B}_{lm}^{-}\hat{\mathcal{R}}_l^{-}(r)), \quad (43)\\ G^{+}(w) &= \sqrt{w^2+\kappa^2}, \quad (44)\\ G^{-}(w) &= \tau_{\mathrm{aw}}w, \quad (45)\end{aligned}$$

$$H(w) = \sqrt{w^2+\kappa^2}+\tau_{\mathrm{aw}}w. \quad (46)$$

Equation (41) is the standard Hankel transform. The relationship of $Y_{lm}(\theta,\psi) = \sqrt{\frac{(2l+1)(l-m)!}{4\pi(l+m)!}}P_{lm}(\theta)\mathrm{e}^{\mathrm{i}m\psi}$ with the standard Legendre function $P_{lm}(\theta)$ is used in this equation. When the colloids are both half-immersed in the air–water interface, i.e., $h=0$, $\partial P_{lm}(z=r_1\cos\theta_1+h=0)/\partial z = \partial P_{lm}(\theta_1=\pi/2)/\partial\theta_1$ and $P_{lm}(z=r_1\cos\theta_1+h=0) = P_{lm}(\theta_1=\pi/2)$.

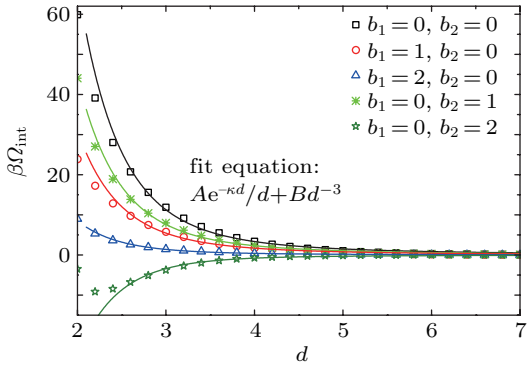


Fig. 6. (color online) The electrostatic pair interaction (hollow symbols) of two like-charged particles trapped in the air–water interface as a function of the dimensionless center–center distance d with different surface distributions. The solid lines are corresponding nonlinear fits (the fit equation is given in the inset). The other parameters are as follows: particle radius $R = 0.5$ μm, total surface charge $Q = 2000$ (in units of unit electric charge), $T = 300$ K, $h = 0$, and the screening length $\kappa^{-1} = 1.06$.

Figure 6 shows the calculation results (denoted by hollow symbols) of the lateral pair interaction, $\beta\Omega_{\mathrm{int}}$, between the particles with radius $R = 0.5$ μm and the total charge $Q = 2000$ for different surface charge distributions. From this figure, we find that the interaction varies quantitatively or even qualitatively with the surface charge distribution. For most situations, there are pure repulsions between two like-charged colloids. While, for the situation of $b_1 = 0$ and $b_2 = 2$, a deep potential well emerges at $d = 2.2$, which indicates a considerable attraction between the particles. It is an interesting result for the potential application in expressing the experimental self-assembly behaviors of the interfacial colloid system in recent years. Ghezzi *et al.*[9,44,51–53] using deionized water found that the polystyrene spheres on a flat water–air interface exhibit spontaneous formations of stable colloid cluster and complicated metastable mesostructures. These experiments revealed the presence of both an attractive primary minimum and an attractive secondary minimum in the effective intercolloidal potential at separations $d < 3.0$ and $d \approx 3.0 \sim 10$, respectively. The weaker attraction with longer interacted range is widely attributed to the long-range capillary force which decays $\propto 1/d$ for non-isolated system.[10,47,54,55] The stronger attraction is generally owing to the competition of the electrostatic repulsion and the van der Waals force. According to the results in Fig. 6, we can now expect that the electrostatic

attraction induced by inhomogeneity of the surface charge on the colloid may be another important reason to cause the primary minimum in the inter-colloidal potential.

As the inter-particle separation is large, the colloids can be considered as point charges. In this situation, the pair interaction energy can be obtained by superpositing the screened Coulomb interaction and the effective dipole–dipole interaction of the counterionic cloud associated with the interfacial colloidal particles. It should have an asymptotic form as reported in Eq. (34) deduced by Hurd. For $d > 2.8$, our results fit well with Hurd's formula (see the solid lines in Fig. 6), which confirms the reliability of our calculation.

3.4. The colloid-orifice member system

The study of the dynamical behavior of the colloid suspension through an orifice or a porous medium, such as electrophoresis and attachment, is of great significance in industry, the environment field, as well as the biological field. This colloid-orifice/porous member system is an interesting model system for fundamental research in contaminant transport, soil profile development, subsurface migration of pathogenic microorganisms, transmembrane transport of biomacromolecules, and so on.[56–60] The fundamental element of the dynamical behavior of this colloid system is obviously the interactions of the colloids and orifice/porous member.

The electrostatic interaction of a colloidal particle restricted by an orifice in a large conducting plane has been investigated in the pioneering work by Keh and Lien.[61] Unfortunately, this analysis was insufficient for the following approximations: i) an assumption of thin double layers adjacent to solid surfaces; ii) neglecting the size effect of charged particle; and iii) a simply homogeneous boundary on the charged particle surface. Now, using the Poisson–Boltzmann theory and considering the size effect of the particle and the exact boundary conditions of the particle surface, we make a systematic examination of the axisymmetric electrostatic interaction of a charged particle creeping along the axis of an orifice in an infinite plane.[62]

Figure 7 shows a simple model of a charged spherical particle with radius R in the vicinity of a plane with a circular orifice of radius h. This particle can creep along the axis of the circular orifice. The system is immersed in an electrolyte with anion and cation of valence z_0, modeled by a dielectric continuum of dielectric constant ε_e. For convenience of calculation, we divide the area outside the particle into two parts: part I corresponds to the region of the electric solution of $z < 0$, including the colloidal particle; part II denotes the region of the electric solution of $z > 0$. Here, the index I (II) will refer to evaluation in the I (II) phase. We denote the boundary with the Cartesian coordinate $z = 0$, $\rho > h$ by S_w (not including the circular orifice), the surface of circular orifice ($z = 0, \rho \le h$) by S_0, and the surface of the particle by S_p. Here, (ρ, z, ψ) and (r, θ, ψ) denote the circular cylindrical coordinates and the spherical coordinates, respectively. The origins of these two coordinates are fixed separately at the sphere center and the orifice center.

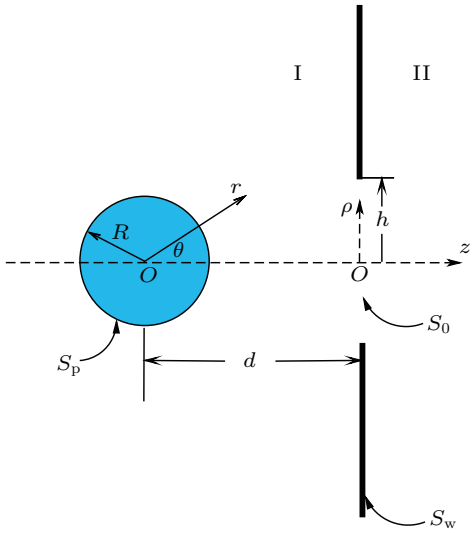


Fig. 7. (color online) A spherical particle creeping along the axis of a circular orifice.

For simplification, we assume the particle to be uniformly charged (the calculation method in the present paper is also available to the nonuniformly charged particles, but we should make a 3D calculation). Since the spherical particle is located on the axis of the circular orifice and is uniformly charged, the system is an axisymmetric one. That is to say, the electric potentials of the system are independent of the rotation angle ψ. Following an idea of the multipole expansion method, the electric potentials Φ_I and Φ_{II} outside the particle and Φ_{in} inside the particle can be expanded in terms of basis functions,

$$\begin{aligned}\Phi_I &= \sum_{s=0}^{+\infty} A_s k_s(\kappa r) P_s(\cos\theta) \\ &\quad + \int_0^{\infty} F(w) w J_0(w\rho)\, \mathrm{e}^{\sqrt{w^2+\kappa^2}z}\, \mathrm{d}w, \\ &\quad s = 0, 1, 2, \ldots, \infty, \end{aligned} \tag{47}$$

$$\Phi_{II} = \int_0^{\infty} G(w) w J_0(w\rho)\, \mathrm{e}^{-\sqrt{w^2+\kappa^2}z}\, \mathrm{d}w, \tag{48}$$

$$\Phi_{in} = \sum_{s=0}^{+\infty} C_s r^s P_s(\cos\theta), \quad s = 0, 1, 2, \ldots, \infty. \tag{49}$$

Two kinds of boundary conditions of the orifice plane are considered in this paper. One is the fixed potential model (corresponding to a conducting plane), and the other is the fixed charge model.

3.4.1. Fixed surface potential model for the surface of the orifice plane

Since the plane extends to infinity and is an equipotential surface, we set the electric potential on S_w as the elec-

tric potential reference point. It should be noticeable that the electric potential at the orifice (the surface of S_0) is not necessary to be zero, which can be defined in a general form as $\Phi_{\rm I}|_{S_{0<}} = \Phi_{\rm II}|_{S_{0>}} = f(\rho)$. Meanwhile, the current flux is continuous for $\rho < h$. The boundary conditions on the surface of the orifice plane then can be summarized as follows:

$$\Phi_{\rm I}(\boldsymbol{r}) = \Phi_{\rm II}(\boldsymbol{r}) = \begin{cases} f(\rho), & \boldsymbol{r} \in S_0, \\ 0, & \boldsymbol{r} \in S_{\rm w}. \end{cases} \tag{50}$$

$$\nabla\Phi_{\rm I}(\boldsymbol{r}) = \nabla\Phi_{\rm II}(\boldsymbol{r}), \quad \boldsymbol{r} \in S_0. \tag{51}$$

Substituting the electric potentials $\Phi_{\rm I}$ and $\Phi_{\rm II}$ into the above boundary conditions and making an Hankel transform, we can express the prefactors $F(w)$ and $G(w)$ as follows:

$$F(w) = -\frac{1}{2}\left[H_1^*(w) + \frac{1}{\sqrt{w^2+\kappa^2}}H_2^*(w)\right], \tag{52}$$

$$G(w) = \frac{1}{2}\left[H_1^*(w) - \frac{1}{\sqrt{w^2+\kappa^2}}H_2^*(w)\right]. \tag{53}$$

Here,

$$H_1^*(w) = \int_0^\infty {\rm d}\rho \sum_{s=0}^\infty A_s k_s(\kappa r) P_s(\cos\theta)\rho J_0(w\rho), \tag{54}$$

$$H_2^*(w) = \int_0^h {\rm d}\rho \sum_{s=0}^\infty A_s \rho J_0(w\rho)\left(k_s'(\kappa r)\kappa P_s(\cos\theta)\cos\theta + k_s(\kappa r)P_s'(\cos\theta)\frac{\sin^2\theta}{r}\right), \tag{55}$$

with $r = \sqrt{d^2+\rho^2}$, $\cos\theta = d/\sqrt{d^2+\rho^2}$, $k_s'(\kappa r) = {\rm d}k_s(x)/{\rm d}x|_{x=\kappa r}$, and $P_s'(\cos\theta) = {\rm d}P_s(x)/{\rm d}x|_{x=\cos\theta}$.

3.4.2. Fixed surface charge model for the surface of the orifice plane

In this case, the normal gradient of the electric potential on the orifice plane is proportional to the surface charge density σ_w. The potential and current flux at the orifice are also continuous.

$$\Phi_{\rm I}(\boldsymbol{r}) = \Phi_{\rm II}(\boldsymbol{r}) = g(\rho), \quad \boldsymbol{r} \in S_{\rm w}, S_0, \tag{56}$$

$$(\nabla\Phi_{\rm I}(\boldsymbol{r}) - \nabla\Phi_{\rm II}(\boldsymbol{r}))\cdot\boldsymbol{n}_w = \begin{cases} \lambda_{\rm B}\sigma_w, & \boldsymbol{r} \in S_{\rm w}, \\ 0, & \boldsymbol{r} \in S_0, \end{cases} \tag{57}$$

where $\boldsymbol{n}_w$ is an outer normal unit vector of surface G_w.

Similarly, we substitute $\Phi_{\rm I}$ and $\Phi_{\rm II}$ into the above boundary conditions and obtain the precise expressions for $F(w)$ and $G(w)$,

$$F(w) = \frac{1}{2}\left[H_3^*(w) - H_4^*(w)\right], \tag{58}$$

$$G(w) = \frac{1}{2}\left[H_3^*(w) + H_4^*(w)\right]. \tag{59}$$

Here,

$$H_3^*(w) = \frac{1}{\sqrt{w^2+\kappa^2}}\left\{\frac{\sigma_w}{w}\left[\delta(w) - hJ_1(hw)\right] - H_4^*(w)\right\}, \tag{60}$$

$$H_4^*(w) = \int_h^\infty {\rm d}\rho \sum_{s=0}^\infty A_s \rho J_0(w\rho)\left(k_s'(\kappa r)\kappa P_s(\cos\theta)\cos\theta + k_s(\kappa r)P_s'(\cos\theta)\frac{\sin^2\theta}{r}\right). \tag{61}$$

Once getting the specific expressions of $F(w)$ and $G(w)$, the electrostatic potential and the interaction energy can be obtained by solving Eqs. (13)–(16) and (18).

Figure 8 shows the interaction energy between the particle and the orifice plane as a function of the particle–orifice distance d for different orifice radius h. To be convenient for comparison between the fixed potential model and the fixed charge model of the orifice plan, we display the results of these models in the same figure. The figure shows significant difference between these two models. There is electrostatic attraction between the particle and orifice plane for the fixed potential model, while it is pure electrostatic repulsion for the fixed charge model. It is a remarkable result because it opens the possibility to manipulate particle–orifice interactions (adsorption and desorption) in a reversible manner by switching the orifice plane condition between fixed potential and fixed surface charge. To check the consistency of our calculations, the analytical result of the electrostatic energy for the same particle normal to an infinite plane (it can be easily solved in the bispherical coordinate) is compared with the results of the limiting case as $h \to 0$. Obviously, they agree well with each other.

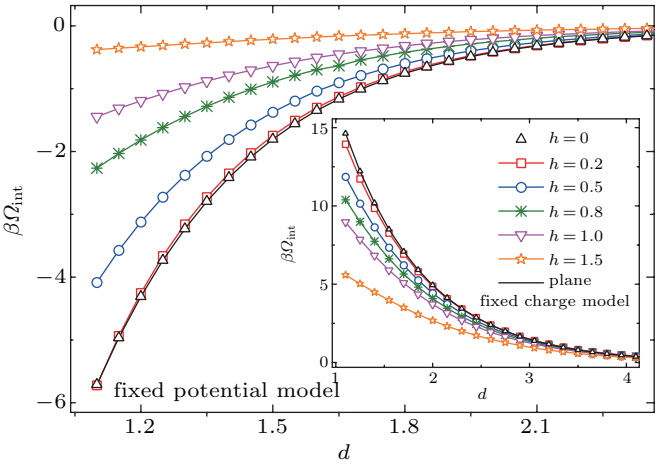


Fig. 8. (color online) Interaction energy of the charged particle and the orifice plane as a function of reduced particle–orifice distance d for different reduced orifice radius h. Two kinds of boundary conditions of the orifice plane are considered: the fixed potential model and the fixed charge model (shown in the inset). The Debye screen length $\kappa^{-1} = 1.195$.

Figure 8 also reveals that the attraction (repulsion) between the particle and the orifice plane for the fixed potential model (fixed charge model) is weakened with the increase of the orifice size h. Obviously, the interaction vanishes as $h \to \infty$. From our calculation, we can find that the interaction is also sensitive to the total charge on the particle, the size of

the particle, and the charge density of the orifice plan.[62] The increases of these parameters enhance the interaction. Meanwhile, the interaction range can be shortened by decreasing the screen length of the water, which can be achieved by increasing the ion concentration c_0 or/and the ion valence z_0 for their relation of $\kappa^{-1} \propto z_0\sqrt{c_0}$.

4. Summary

In this paper, we present a semi-analytical method to calculate the electrostatic interaction of the spherical colloids by combining the analytical expansion of the basic functions and the coordinate translation-rotation transform and the numerical multipoint collection method. We have successfully applied the method into an unconfined diluted colloid solution and many confined cases such as long cylindrical wall confinement, the air–water interfacial confinement and porous membrane confinement. "Like-charged" attractions are found between the particles when the particles were nonuniformly charged for both unconfined and confined systems. Furthermore, we systematically analyzed the effectiveness of sensitive parameters to the interaction energy of the system. For every application, we have made consistence checks of our calculation with some known analytical cases. The distribution of the charge on the particle surface can be uniform or nonuniform in our given applications. In fact, our method has no constraint on the surface charge distribution of the particle. Moreover, in theory, the method in the present paper is available for any dilute colloid solution with a regular solid confinement such as spherical cavity confinement and lamellar confinement. Consequently, there is still a wide potential application in the colloidal system. Finally, we should note that the colloid particle should be weakly charged in our method, such that the superposition approximation applied in Eqs. (4) and (5) is reliable. However, for the strongly charged colloid or the concentrated colloid solution, the nonlinear effect should be considered in electrostatic potentials.

References

[1] Eldridge M, Madden P and Frenkel D 1993 *Nature* **365** 35
[2] Cottin X and Monson P A 1995 *J. Chem. Phys.* **102** 3354
[3] Bolhuis P G and Kofke D A 1996 *Phys. Rev. E* **54** 634
[4] Zhao D, Long L and Xiao C 2010 *Chin. Phys. B* **19** 0128203
[5] Li J, Wen K, He W, Wang X, Lv W, Yan P, Song Y, LU H, Lin X and Dickerson J H 2014 *Chin. Phys. B* **23** 56103
[6] Li W and Xiu F 2010 *Chin. Phys. B* **19** 108204
[7] Wang J, Yuan C and Tong F 2005 *Chin. Phys. B* **14** 1581
[8] Marcus A H and Rice S A 1996 *Phys. Rev. Lett.* **77** 2577
[9] Chen W, Tan S, Ng T K, Ford W T and Tong P 2005 *Phys. Rev. Lett.* **95** 218301
[10] Nikolaides M, Bausch A, Hsu M, Dinsmore A, Brenner M, Weitz D and Gay C 2002 *Nature* **420** 299
[11] Wu Y, Chen C, Xu X, Liu Y, Shao W, Yin N, Zhang W, Ke J and Fang X 2014 *Chin. Phys. B* **23** 088703
[12] Eral H B, Oh J M, van den Ende D, Mugele F and Duits M H G 2010 *Langmuir* **26** 16722
[13] Sophie C. Shen, Liu W and Diao J 2015 *Chin. Phys. B* **24** 0127308
[14] Zhao Y, Li Juan, Liu Q, Dong W, Chen B and Li C 2015 *Chin. Phys. B* **24** 028104
[15] Zheng B and Meng Q 2014 *Chin. Phys. B* **23** 038701
[16] Huang L, Xiao C, Hu P, Gao H 2009 *Chin. Phys. B* **18** 01287
[17] Wang A, Chen S, Dong P, Zhou Q, Yuan G and Su G 2009 *Chin. Phys. Lett.* **26** 86104
[18] Derjaguin B V and Landau L 1993 *Prog. Surf. Sci.* **43** 30
[19] Verwey E J W and Overbeek J T G 1948 *Theory of the Stability of Lyophobic Colloids* (Amsterdam: Elsevier)
[20] Crocker J C and Grier D G 1996 *Phys. Rev. Lett.* **77** 1897
[21] Crocker J C and Grier D G 1994 *Phys. Rev. Lett.* **73** 352
[22] Larsen A E and Grier D G 1997 *Nature* **385** 230
[23] Carnie S L, Chan D Y C and Stankovich J 1993 *J. Colloid Interface Sci.* **155** 297
[24] Carnie S L and Chan D Y C 1994 *J. Colloid Interface S* **165** 116
[25] Stankovich J and Carnie S L 1996 *Langmuir* **12** 1453
[26] Ospeck M and Fraden S 1998 *J. Chem. Phys.* **109** 9166
[27] Bowen W R and Sharif A O 1998 *Nature* **393** 663
[28] Neu J C 1999 *Phys. Rev. Lett.* **82** 1072
[29] Trizac E and Raimbault J L 1999 *Phys. Rev. E* **60** 6530
[30] Sader J E and Chan D Y C 2000 *Langmuir* **16** 324
[31] Chen W and Tong P 2008 *Europhys. Lett.* **84** 28003
[32] Zhou Y and Ng T K 2007 arXiv:cond-mat/0703667
[33] Lian Z and Ma H 2008 *J. Phys.: Condens. Matter* **20** 035109
[34] Lian Z and Ma H 2007 *J. Chem. Phys.* **127** 104507
[35] Crocker J C and Grier D G 1996 *Phys. Rev. Lett.* **77** 1897
[36] Grier D G and Han Y 2004 *J. Phys.: Condens. Matter* **16** S4145
[37] Han Y and Grier D G 2003 *Phys. Rev. Lett.* **91** 038302
[38] Polin M, Grier D G and Han Y 2007 *Phys. Rev. E* **76** 041406
[39] Pieranski P 1980 *Phys. Rev. Lett.* **45** 569
[40] Masschaele K, Park B J, Furst E M, Fransaer J and Vermant J 2010 *Phys. Rev. Lett.* **105** 048303
[41] Wirth C L, Furst E M and Vermant J 2014 *Langmuir* **30** 2670
[42] Hurd A J 1985 *J. Phys. A: Math. Gen.* **18** L1055
[43] Frydel D and Dietrich S 2007 *Phys. Rev. Lett.* **99** 118302
[44] Stamou D, Duschl C and Johannsmann D 2000 *Phys. Rev. E* **62** 5263
[45] Lehle H, Oetel M and Dietrich S 2006 *Europhys. Lett.* **75** 174
[46] Foret L and Würger A 2004 *Phys. Rev. Lett.* **92** 058302
[47] Oettel M, Domínguez A and Dietrich S 2005 *J. Phys.: Condens. Matter* **17** L337
[48] Würger A 2005 *J. Phys. Chem. B* **109** 16435
[49] Park B J, Lee M, Lee B and Furst E M 2015 *Soft Matter* **11** 8701
[50] Lian Z 2016 *J. Chem. Phys.* **145** 014901
[51] Ghezzi F, Earnshaw J, Finnis M and McCluney M 2001 *J. Colloid Interface Sci.* **238** 433
[52] Ruiz-García J, Gámez-Corrales R and Ivlev B 1998 *Phys. Rev. E* **58** 660
[53] Quesada-Pérez M, Moncho-Jordá A, Martnez-López F and Hidalgo-álvarez R 2001 *J. Chem. Phys.* **115** 10897
[54] Domínguez A, Oettel M and Dietrich S 2005 *J. Phys.: Condens. Matter* **17** S3387
[55] Würger A 2005 *J. Phys. Chem. B* **109** 16435
[56] Torkzaban S, Bradford S A, van Genuchten M T and Walker S L 2008 *J. Conta. Hydrology* **96** 113
[57] McGechan M and Lewis D 2002 *Biosystems Engineering* **82** 1
[58] Bradford S A, Simunek J, Bettahar M, van Genuchten M T and Yates S R 2003 *Environ. Sci. Technol.* **37** 2242
[59] Bringuier E and Bourdon A 2003 *Phys. Rev. E* **67** 011404
[60] Ito Y and Park Y S 2000 *Polym. Adv. Technol.* **11** 136
[61] Keh H J and Lien L C 1991 *J. Fluid Mech.* **224** 305
[62] Lian Z 2010 *Chin. Phys. B* **19** 058202